



HAL
open science

Science with MATISSE

Sebastian Wolf, Bruno Lopez, J. -Ch. Augereau, Marco Delbo, Carsten Dominik, Th. Henning, K. -H. Hofmann, Michiel Hogerheijde, Josef Hron, Walter Jaffe, et al.

► **To cite this version:**

Sebastian Wolf, Bruno Lopez, J. -Ch. Augereau, Marco Delbo, Carsten Dominik, et al.. Science with MATISSE. SPIE Astronomical Telescopes + Instrumentation, Jun 2016, Edinburgh, France. pp.99073S, 10.1117/12.2232835 . hal-03539954

HAL Id: hal-03539954

<https://hal.science/hal-03539954v1>

Submitted on 18 Jan 2025

HAL is a multi-disciplinary open access archive for the deposit and dissemination of scientific research documents, whether they are published or not. The documents may come from teaching and research institutions in France or abroad, or from public or private research centers.

L'archive ouverte pluridisciplinaire **HAL**, est destinée au dépôt et à la diffusion de documents scientifiques de niveau recherche, publiés ou non, émanant des établissements d'enseignement et de recherche français ou étrangers, des laboratoires publics ou privés.

Science with MATISSE

Sebastian Wolf^a, Bruno Lopez^b, Jean-Charles Augereau^c, Marco Delbo^b, Carsten Dominik^d, Thomas Henning^e, Karl-Heinz Hofmann^f, Michiel Hogerheijde^g, Josef Hron^h, Walter Jaffe^g, Thierry Lanz^b, Klaus Meisenheimer^e, Florentin Millour^b, Eric Pantinⁱ, Roman Petrov^b, Dieter Schertl^f, Roy van Boekel^e, Gerd Weigelt^f, Andrea Chiavassa^b, Attila Juhasz^j, Alexis Matter^b, Anthony Meilland^b, Nicolas Nardetto^b, and Claudia Paladini^k

^aUniversität zu Kiel, Institut für Theoretische Physik und Astrophysik, Leibnizstr. 15, 24098 Kiel, Germany

^bLaboratoire Lagrange, UMR7293, Université de Nice Sophia-Antipolis, CNRS, Observatoire de la Côte d'Azur, Nice, France

^cUJF-Grenoble 1/CNRS-INSU, Institut de Planétologie d'Astrophysique de Grenoble (IPAG) UMR 5274, Grenoble, 38041, France

^dSterrenkundig Instituut "Anton Pannekoek", Science Park 904, 1098 XH, Amsterdam, The Netherlands; Afdeling Sterrenkunde, Radboud Universiteit Nijmegen, Postbus 9010, 6500 GL, Nijmegen, The Netherlands

^eMax-Planck-Institut für Astronomie, Königstuhl 17, 69117 Heidelberg, Germany

^fMax-Planck-Institut für Radioastronomie, Auf dem Hügel 69, 53121 Bonn, Germany

^gSterrewacht Leiden, Universiteit Leiden, Niels-Bohr-Weg 2, 2300 CA, Leiden, The Netherlands

^hInstitut für Astronomie, Universität Wien, Türkenschanzstraße 17, 1180 Wien, Austria

ⁱCEA/DSM/IRFU/Service d'Astrophysique, CE Saclay, France

^jInstitute of Astronomy, University of Cambridge, Madingley Road, Cambridge, CB3 0HA, United Kingdom

^kInstitut d'Astronomie et d'Astrophysique, Université libre de Bruxelles, Boulevard du Triomphe CP 226, B-1050 Bruxelles, Belgium

ABSTRACT

We present an overview of the scientific potential of MATISSE, the Multi Aperture mid-Infrared Spectroscopic Experiment for the Very Large Telescope Interferometer. For this purpose we outline selected case studies from various areas, such as star and planet formation, active galactic nuclei, evolved stars, extrasolar planets, and solar system minor bodies and discuss strategies for the planning and analysis of future MATISSE observations. Moreover, the importance of MATISSE observations in the context of complementary high-angular resolution observations at near-infrared and submillimeter/millimeter wavelengths is highlighted.

Keywords: Astrophysics, Long-baseline interferometry, Infrared, Very Large Telescope Interferometer, MATISSE

1. INTRODUCTION

MATISSE, the Multi Aperture Mid-Infrared Spectroscopic Experiment,¹ is foreseen as a mid-infrared spectro-interferometer combining the beams of up to four Unit telescopes (UTs) or Auxiliary telescopes (ATs) of the Very Large Telescope Interferometer (VLTI). MATISSE will measure closure phase relations and thus offer an efficient capability for image reconstruction. MATISSE will open two new observing windows at the VLTI: The L and M bands in addition to the N band with the possibility to perform simultaneous observations in separate bands. MATISSE will be equipped with several spectroscopic modes with spectral resolutions up to ~ 5000 .

Further author information: Send correspondence to S. Wolf (wolf@astrophysik.uni-kiel.de)

These modes will provide unique insight in the physical properties and kinematics of line emitting gas regions, for example in the environment of young stellar objects (YSOs) and hot stars.

MATISSE will extend the astrophysical potential of the VLTI in the mid-infrared wavelength range by overcoming the ambiguities often existing in the interpretation of simple visibility measurements. The existence of the four large apertures of the VLTI will permit to push the sensitivity limits up to values required by selected astrophysical programs such as the study of Active Galactic Nuclei and protoplanetary disks around low-mass stars. Moreover, the existence of the ATs which are relocatable in position will allow the exploration of the Fourier plane with up to 200 meters baseline length. Key science programs using the ATs cover for example the formation and evolution of planetary systems, the birth of massive stars as well as the observation of the high-contrast environment of hot and evolved stars.

In most astrophysical domains which require a multi-wavelength approach, MATISSE will be a perfect complement to other high angular resolution facilities. MATISSE covers the mid-infrared spectral domain, between the near-infrared domain, for which various high-angular resolution instruments are available (e.g., SPHERE/VLT, PIONIER/VLTI) and submillimeter/millimeter wavelengths at which ALMA, the Atacama Large Millimeter Array, operates. With the extended wavelength coverage from the L to the N band, MATISSE will not only allow one to trace different spatial regions of the targeted objects, but also different physical conditions and processes as well as the possibly varying origin of the radiation (thermal radiation vs. scattered light) and thus provide insights into previously unexplored areas, such as the investigation of the distribution of volatiles in addition to that of the dust.

In the following science cases for MATISSE from the fields of star and planet formation (Sect. 2), stellar physics (Sect. 3), planetary systems (Sect. 4), and Active Galactic Nuclei (Sec. 5) are presented.

2. PHYSICS OF STAR AND PLANET FORMATION

2.1 Class II YSOs / gas-rich disks

The circumstellar disks around newly-formed stars have been subject to intense study for decades. Their structure and chemical composition are interesting because they are the birth places of new planetary systems. Determining the properties of the “building material” for planets, as well as measuring signatures of interaction between planets and the disk material, provide much needed observational constraints on models of disk evolution and planet formation. However, the small angular scales involved pose technological challenges: at a distance of 150 pc, typical for nearby young stars, the orbital radius of Jupiter corresponds to only $0''.035$. This makes direct study of the disks at these scales the realm of interferometers. The innermost ≈ 15 au of the disks are the most interesting in terms of planet formation on solar system scales. These can be well observed in the near- and thermal infrared where we predominantly trace the warm surface layer of the disks. For an overview of science cases for next-generation optical/infrared long-baseline interferometers in the field of circumstellar disks and planets see.²

In this section we present some of the capabilities of MATISSE for studying disks of “intermediate” age that are commonly referred to as “class II” objects.³ They are typically 1 to a few million years old, and contrary to the younger “class I” objects they are no longer deeply embedded in their natal clouds. The class II disks are still relatively massive and gas-rich, with typical disk/star mass ratios of order 10^{-2} and at least an order of magnitude scatter around this value.⁴ Most T Tauri and Herbig Ae (HAe) stars are class II objects. They are thought to be the predecessors of the debris disk objects that have lost their primordial gas and dust and have much less massive disks of secondary dust, produced in collisional grind-down of larger bodies. The class II phase lasts a few million years,⁵ during which there is typically still substantial accretion onto the central star at rates approximately following the relation $\dot{M} \approx 10^{-8} (M_*/M_\odot)^2$, where \dot{M} is the accretion rate in M_\odot/yr and M_* denotes the stellar mass, with about two orders of magnitude scatter about this average relation.⁶⁻⁸ The class II phase is thought to be the main phase of planet formation in the “core accretion paradigm”,⁹ and at least gas giant planet formation must be completed before the gaseous disk has dissipated.

The spatial structure of the disks around T Tauri and HAe stars has been intensively studied in order to constrain the evolution of the disks that finally leads to their dissipation, and to search for signatures of forming planets and their interaction with the disk material. Because the angular extent of the disk emission is small,

this has been the realm of interferometers. At different wavelengths we see physically different parts of the disk. In the near-infrared we can observe thermal emission from material in the very inner disk, typically at less than 1 au from the star. Around $10\ \mu\text{m}$ we see a larger region of order 10 au in size for a typical HAe star* that originates in the warm disk surface layer. At millimeter wavelengths we mostly see the cooler disk interior, and can observe emission out to >100 au, provided the disk has an appreciable optical depth at these large radii. Typical apparent sizes for a disk around a HAe star at a distance of 150 pc are <10 mas for the thermal emission in the H and K bands, $\approx 0''.1$ at $10\ \mu\text{m}$, and up to a few arcseconds for the emission at millimeter wavelengths.¹⁰ In addition to the thermal disk emission we may observe stellar light scattered off dust grains in the disk surface out to >100 au,^{11,12} and in some cases we may observe emission from stochastically heated particles like Polycyclic Aromatic Hydrocarbons (PAHs).¹³

It has become apparent that the class II disks show much structure, such as gaps and rings in the large grain distribution near the midplane as seen in millimeter observations^{14–16} and in scattered light,^{17,18} and large scale spirals seen in scattered light observations.^{19,20} In the innermost few au of several disks evidence for gaps was found using infrared interferometry, in particular combining near-infrared and $10\ \mu\text{m}$ observations.^{21–23}

2.1.1 The MIDI heritage

The MIDI instrument at the VLT Interferometer²⁴ was the predecessor of MATISSE operating at $10\ \mu\text{m}$. It was a two-element optical interferometer, capable of spectrally resolved measurements between 8 and $13\ \mu\text{m}$. It was the first facility that allowed systematic investigation of disks at these wavelengths with a spatial resolution of $\lesssim 10$ mas, corresponding to a linear resolution close to 1 au at a distance of 150 pc. MIDI saw first light in December 2002 and in the 12 years of regular observations that followed well over 100 disks were studied. These experiments resulted in numerous new insights, such as a correlation between spatial extent of the disk emission and SED shape,²⁵ radial gradients in dust composition,^{26,27} the detection of gaps,^{21–23} and the detailed measurement of the “wall” shape in transition disks.^{28,29}

The largest and most systematic analysis of the disk observations performed with MIDI was recently presented.³⁰ The key results of this study are summarized in Fig. 1, where the MIDI size-color diagram of the studied sample of HAe star disks is shown. In the vertical direction sources go from compact to extended (bottom to top), in the horizontal direction from blue to red (left to right). The “shark fin-shaped” regions show the ranges occupied by radiative transfer models of disks.³⁰ The grey region shows the range occupied by continuous, gap-less models. The larger yellow region shows where radiative transfer models with a range of gap sizes lie. It was found that:

1. Sources group I-type[†] SEDs³¹ (traditionally associated with flared disk geometries, green symbols in Fig. 1) show evidence of large gaps in the spatially resolved data, confirming an earlier hypothesis;
2. Many sources with group II-type SEDs (traditionally thought to have flat disks, red symbols in Fig. 1) have the signature of a continuous, “gap-less” disk, but
3. Some group II sources do show evidence for (smaller) gaps in their inner disk regions.

The emergent picture is that the signatures of radial gaps are much more common among HAe star disks than previously thought. Should these gaps be caused by planet-disk interaction, then planets of ≈ 1 Saturn mass or more must be very common in these young disks, opening exciting prospects of detecting and characterizing them with e.g. METIS³² at the E-ELT. In particular, the discovery of group II sources with gaps is exciting; these gaps are too small to be noticeable in the SED and could only be uncovered with the high spatial resolution that MIDI offered. With MIDI we could demonstrate the presence of gaps in the inner disks of many objects. With MATISSE we can take the next step and accurately measure the gap profiles and possibly detect small-scale asymmetries.

The thermal emission of disks arises from dust grains that are in equilibrium with the radiation field. The spatial extent of the region we see at a given wavelength is that where the temperature is high enough for the Planck function to not be deeply in the Wien regime. The size of this region scales approximately with $\sqrt{L_\lambda^2}$, where L_* is the stellar luminosity and λ the observing wavelength.

[†]Note that the group I vs. group II classification³¹ is an SED-based sub-division of the optically visible, gas-rich disks. Both group I and group II sources are class II³ objects.

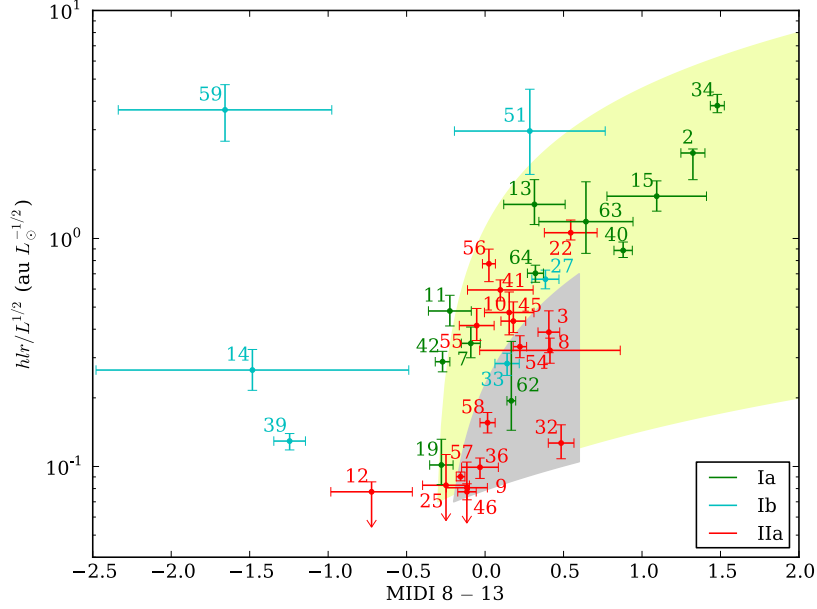


Figure 1. The MIDI size-color diagram for Herbig Ae star disks (figure adopted from³⁰).

2.1.1.2 The future: MATISSE

The MIDI data revealed a large diversity of inner disk geometries. However, due to the limited capabilities of MIDI (1 simultaneous baseline, no closure phases, only N band), the geometry of the inner disks and gaps could be studied in little detail only. Taking the next step requires the qualitatively new capabilities of MATISSE.¹ With its four-element beam combiner it delivers 6 baselines as well as 3 independent closure phases with each individual measurement. This yields qualitatively new observational possibilities:

- Precise mapping of the radial intensity profiles, localizing gaps and measuring their shapes,
- Measurement of inner disk inclinations and position angles,
- Sensitive measurement of deviations from point symmetry using closure phases,
- Higher resolution mapping of the inner ≈ 1 au using the 3-5 μm spectral range,
- Measurement of the gas kinematics in the inner disk and accretion columns (see Sect. 2.2), and
- Model-independent image re-construction.

Exquisite survey power The inner disks can be surveyed for signatures of gaps or asymmetries with a single or few measurements per source, allowing to efficiently identify objects exhibiting sub-structure, which can then be followed-up with better UV coverage and be mapped in detail. The large wavelength range (3-14 μm) allows probing the disk from $\lesssim 1$ au to ≈ 10 au. The availability of an external fringe tracker is essential for surveys because it allows larger samples of objects to be observed with the ATs.

Model-independent image re-construction MATISSE was designed to allow model-independent image re-construction by measuring visibility amplitudes and closure phases at a broad range of different baselines. The re-configurable ATs are essential to sample both the low spatial frequencies with a compact configuration as well as the high spatial frequencies on longer baselines. Also here, an external fringe tracker is essential for image re-construction experiments because the required UV coverage can only be achieved with the ATs.

In Fig. 2 we show an example of a MATISSE image re-construction experiment, targeted at the transition disk object HD 179218. The left panel shows a radiative transfer model that provides a good fit to a set of 18 MIDI observations (Menu et al., *subm.*). The MIDI data indicate a large gap with a radius of 10 au, a small

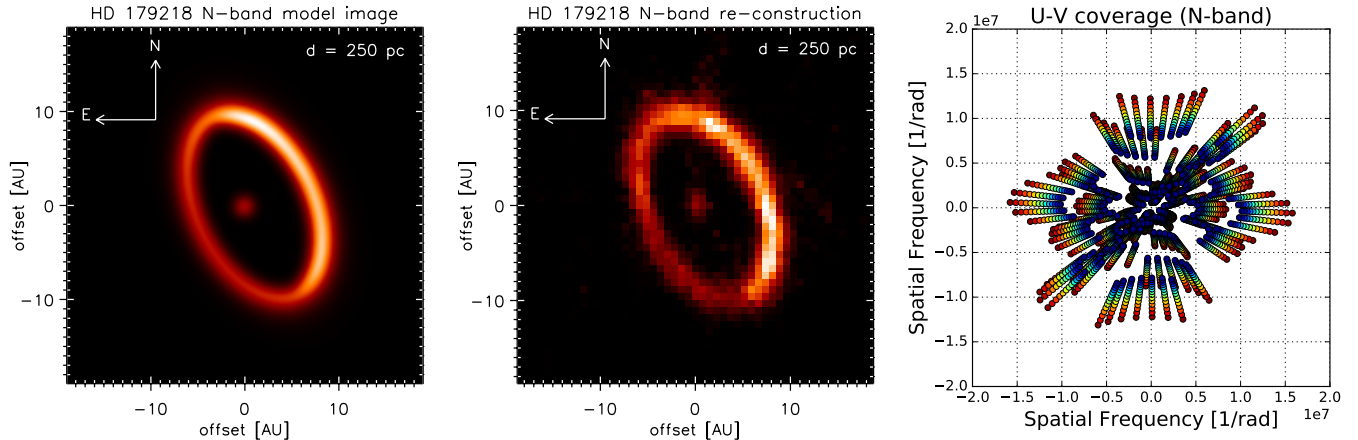


Figure 2. An image re-construction experiment using simulated MATISSE data of the transition disk HD 179218. *Left*: radiative transfer model image; *center*: re-constructed Matisse image; *right*: UV coverage.

amount of spatially unresolved warm dust around the star, and a slightly eccentric gap shape. The middle panel shows an image that was re-constructed from simulated MATISSE observations using the software SQUEEZE[‡], on 3 AT configurations and with 7 measurements per configuration[§]. In this experiment an average N band image was made from a series of monochromatic images in the 8-13 μm range, and data in the whole wavelength range were used together in the re-construction of a single, average image. Methods for simultaneous multi-wavelength re-construction are being developed and should in time replace this simplified approach.

2.2 Observing molecular line radiation from protoplanetary disks

MATISSE not only promises a rich discovery space for observations of the thermal emission of dust grains in planet-forming disks, but is also capable of detecting spectral lines at resolutions up to 3500 (M-band) to 5100 (L-band). Corresponding to velocity resolutions of $<100 \text{ km s}^{-1}$, such observations promise to reveal key astrophysical processes related to the forming star: Atomic lines such as Br γ and Pf β trace accretion from the disk onto the star as well as high velocity winds and jets driven by the star.³³⁻³⁶ The spatial resolution of MATISSE of 0.5–1.0 au in typical nearby star forming regions provides strong constraints on geometry of accretion and the launch points of the winds and jet.

In the M-band, MATISSE offers the unique capability to obtain high angular resolution observations of the ro-vibrational ground state lines of CO, around 4.67 μm . The lines, distributed over a *P* and *R* branch, are separated by $\sim 0.04 \mu\text{m}$ (2500 km s^{-1}). At a resolution $R \sim 3500$ MATISSE can easily separate the individual rotational lines. High velocity (tens to a few hundred km s^{-1}) emission of CO is expected to trace the disk winds if they are launched near the inner edge of the disk. Together with the atomic lines described above, MATISSE is likely to offer important insight into the wind/jet driving mechanism, which is an essential process in the star formation that regulates the angular momentum of the accreting star.

The CO ro-vibrational ground state lines have been extensively studied at very high spectral resolution ($R \sim 100,000$) using long-slit spectroscopy with VLT/CRIRES and Keck/NIRSPEC.³⁷⁻⁴² These observations do not spatially resolve the emission, but from the resolved line profiles the emission is found to originate from the inner 0.1 au of the disk. The occurrence of these lines suggests that the inner disks, even if cleared out of dust, still hold (some) gas. The latter explains the continued accretion that is observed onto these stars. However, the mechanism through which gas can filter through the inner disk holes is unknown. Does gas uniformly fill the hole, suggesting that (some) gas can filter past the inner dust disk edge? Or is gas subject to dynamical

[‡]<https://github.com/fabienbaron/squeeze>

[§]The re-constructed image was obtained using a pixel scale of 3 mas. The L0-norm was used as regularizer and the value of the hyper parameter μ was set to 10000. No a-priori assumption on the target's brightness distribution was made. The resulting image that fits the simulated V^2 and closure phases with a total $\chi^2=1.5$.

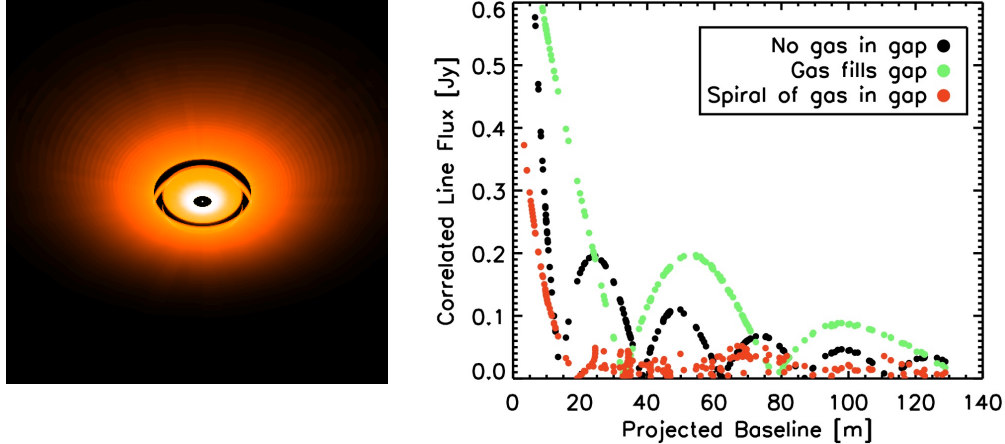


Figure 3. Left: Simulated image of a Herbig Ae disk with a cleared out gap, seen under an inclination of 45° . Right: Predicted correlated flux in CO-line emission channels for three different models: with no gas in the gap (black symbols), with the gap uniformly filled with gas (green symbols), and with a spiral streamer of gas in the otherwise empty gap (red symbols).

interaction with a planet/companion in the hole, forming a spiral accretion flow onto the star (or even onto the planet)?

The MATISSE M-band resolution of 3500 will allow us to separate the individual rotational lines of the CO P- and R-branches of the ro-vibrational ground-state spectrum from the intervening continuum. MATISSE will not velocity-resolve the individual lines, which NIRSPEC and CRIRES observations show to extend to 100 km s^{-1} or less. By studying the differential visibilities between the continuum and the CO lines, we will be able to investigate if (a) a hole is present in CO just like the hole seen in continuum, or (b) the gas uniformly fills the hole. Furthermore, the closure phases provided by MATISSE will immediately tell us if the CO emission is symmetric or confined to asymmetric structures such as spiral arms. Figure 3 illustrates the three different scenarios.

To assess the feasibility of using MATISSE to study the CO ro-vibrational emission from disks, we performed simulations based on simple physical descriptions of the disk and calculated synthetic visibilities. These calculations show that MATISSE has sufficient sensitivity to detect the CO visibilities for a handful of bright Herbig systems, using the UT telescopes. The AT telescopes lack collecting area for this work, and the lower mass (and less bright) T Tauri disks are too weak to be detected even on the UTs. However, a small sample of Herbig systems with disks that are very well studied (and that will most certainly be the subject of continuum work with MATISSE as well) will allow us to address the relative distribution of dust and molecular gas in the inner disk of these representative systems.

Absorption by atmospheric CO is a major complication in these MATISSE observations. The very high resolution CRIRES and NIRSPEC observations described above use the Doppler shift of the source at different epochs to remove the atmospheric absorption from the source emission. At the lower spectral resolution of MATISSE, source emission and atmospheric absorption always coincide in the same spectral resolution element. A careful observational setup is therefore required, that also includes observing a strong calibration source with a featureless spectrum, to characterize the atmospheric absorption. Since the atmospheric absorption occurs in a smooth screen, the relative absorption depth follows from the differential visibilities between the pure-continuum and line-containing spectral channels obtained toward the calibrator. The additional differential visibilities between pure-continuum and line-containing spectral channels toward the source correspond to real structure in the CO emission lines. With detailed model calculations based on the known (spectrally resolved, spatially unresolved long-slit) spectra, specific spatial distributions of CO can then be confirmed or rejected, such as gas filling the gap uniformly or in a spiral arm.

With its unprecedented combination of angular and spectral resolution, MATISSE will offer important new

insight on the relative distributions of dust and gas in the inner disk regions. With MATISSE we can answer important questions, such as how gas accretes from the inner disk edge onto the star and/or possible (planetary?) companions and what the launching region and mechanism is of the powerful jets and winds driven by forming stars.

3. STELLAR PHYSICS

Besides the investigation of the gas/dust phase of protoplanetary disks, MATISSE will also offer the rare opportunity to image the dust around stars, right at the location where it forms. This will allow one to put constraints on the circumstellar structure, on the mass ejection and reorganization, and on the nature and formation processes of dust. MATISSE measurements will be pivotal for the understanding of large multiwavelength datasets on the same targets collected through various high-angular resolution and high-spectral resolution facilities at ESO, covering the infrared to millimeter wavelength range (e.g., near-infrared adaptive optics: NACO, SPHERE; long-baseline interferometry in the near-infrared: PIONIER, GRAVITY; near/mid-infrared spectroscopy: CRILES; mid-infrared imaging: VISIR; submillimeter/millimeter interferometry: ALMA). Among main-sequence and evolved stars, several cases of interest have been identified that are described briefly in the following (see also^{43,44} for an overview of the most important scientific results and open questions):

3.1 Massive stars

Stars with masses $> 8 M_{\odot}$ evolve fast and blast as supernovae at the end of their lives, not without having gone through a firework of different physical processes. Here, we will focus on a selected cases of the various kinds of massive stars:

Dusty blue supergiant stars Several blue supergiant stars produce large amounts of dust before exploding as supernovae. Though they are not the main dust-producers in our Galaxy, they do vastly influence their surroundings by releasing kinetic energy and dust in their vicinity. In some cases, they can even trigger star formation.

The circumstellar environment around Blue supergiant stars is often dense and highly anisotropic. Such a break of symmetry has strong implications on the later phases of stellar evolution, as it can affect the stellar angular momentum. This anisotropy could be driven either by fast-rotation and/or by the presence of a companion star. MATISSE will allow the detection of previously unseen companion stars and the characterization of the gas and dust in the circumstellar environment.

Red supergiant stars Besides their blast as supernova, Red supergiants (RSGs) are also contributors to the chemical and dust enrichment of the Galaxy through their intense mass-loss. As RSGs are not experiencing flares nor pulsations, the triggering of their mass loss remains a mystery and may be linked to the magnetic activity, the stellar convection, and the radiation pressure.

The molecular gas and dust around these stars can be detected best by MATISSE thanks to its wavelength range and angular resolution. MATISSE will provide a full view of the stellar dynamics from the inner part of the photosphere to the outer envelope layers to understand the mass loss mechanism.

3.2 Lower mass stars: AGB & pulsating stars

AGB stars Most of the low and intermediate mass stars end their lives on the Asymptotic Giant Branch (AGB) phase. During this phase, pulsation and radiation pressure on dust leads to a phase of strong mass loss, during which gas and dust enriched by the products of the stellar nucleosynthesis will be ejected. This mass loss is crucial for the chemical enrichment of the interstellar medium and therefore for the chemical evolution of galaxies. A pivotal aspect of the mass-loss process is its geometry, i.e. the density distribution of the circumstellar envelope of the AGB stars at different scales and different evolutionary phases.

To understand the mass-loss process, it is essential to study the mass-loss from very deep inside the star up to the interface with the interstellar medium. Due to its broad wavelength coverage, MATISSE is a unique instrument to study the different dust and molecular species present in the atmospheres and envelopes of AGB stars. The aim is to achieve a complete view from the upper photosphere to the outer envelope layers and to complement Herschel and MIDI surveys.

Envelopes around Cepheids Envelopes around Cepheids have been discovered with long-baseline interferometry in the K Band with the VLTI and CHARA.^{45,46} Since then, four Cepheids have been observed in the N band with VISIR and MIDI⁴⁷⁻⁴⁹ and one with NACO.⁵⁰ Some evidence has also been found using high-resolution spectroscopy.^{51,52} The size of the envelope seems to be at least 3 stellar radii and the flux contribution in K band is from 2% to 10% of the continuum, for medium- and long-period Cepheids respectively, while it amounts to $\sim 10\%$ or more in the N band.

MATISSE offers a unique opportunity to study the envelopes of Cepheids. Determining the size of these envelope (as a function of the spectral band) and their geometry (as a function of the pulsation phase), will bring insights in the links between pulsation, mass loss and envelopes. The impact of CSEs on the period-luminosity relation of Cepheids can also be established.

4. PLANETARY SYSTEMS

4.1 Extrasolar planets

Since the discovery of 51 Peg b, the presence of Jupiter-mass planetary companions at short (< 1 au) orbital distances has raised speculations about their formation and evolution mechanisms. The mid-infrared spectral domain is well adapted to the observation of close-in or young Extrasolar Giant Planets (EGPs). Due to their high effective temperature, these sources are significantly luminous in this wavelength domain. Atmospheric composition, planetary mass, and orbit inclination of extrasolar planets around nearby stars may be studied using IR interferometry at the VLTI.⁵³⁻⁵⁵ Direct characterization of known EGPs can be imagined with the MATISSE instrument by using differential phase and closure phase. Assuming (i, j) the pair of telescopes i and j , the approximated expression of the differential phase produced by a close-in EGP is:

$$\phi_{ij}(\lambda) \simeq \frac{I_{\text{planet}}(\lambda)}{C_*(u_{ij})I_{\text{star}}(\lambda)} \sin(2\pi u_{ij} \cdot \rho), \quad (1)$$

$I_{\text{star}}(\lambda)$ and $I_{\text{planet}}(\lambda)$ are the monochromatic fluxes of the two components, ρ is the angular separation, $C_*(u_{ij})$ is the modulus of the intrinsic visibility of the stellar component with $u_{ij} = B_{ij}/\lambda$ (B_{ij} : baseline between telescopes i and j). The associated closure phase on a closed triplet of baselines is:

$$\Phi_{ij}(\lambda) = \sum_{i,j} \phi_{ij}(\lambda). \quad (2)$$

Several EGP candidates could be foreseen for observations with MATISSE using differential phase and closure phase observables. Fig. 4 and Fig. 5 show the expected differential phases and closure phases for two favourable close-in EGPs detected by radial velocimetry, Gliese 86b ($M \geq 4 M_J$, 0.11 au semi-major axis),⁵⁶ and τ Boo b ($M \simeq 5.8 M_J$, 0.046 au semi-major axis).⁵⁷

The tentative exoplanet programs on VLTI/AMBER and MIDI paved the way to MATISSE. In particular, we managed to strip down the precision of measurements to a few tenths of milliradian on Gliese 86b,⁵⁸ but did not succeed yet to lower the accuracy enough. In such a context, MATISSE has features which make it particularly attractive for the observation of close-in EGPs :

- Observations in the L, M and N bands potentially yield the best possible ratio between the flux expected from an EGP and its star (up to 10^{-3} in the case of Gliese 86b and τ Boo b),
- The error resulting from the still relatively limited background in L band is low enough to get high precision on phase measurements,
- Observations in the L, M, and N bands are intrinsically less affected by infrastructure perturbations than observations at shorter wavelengths,
- The use of four telescopes increases the available closure phases by a factor of four and the available differential phases by a factor of two, if compared to the AMBER instrument.

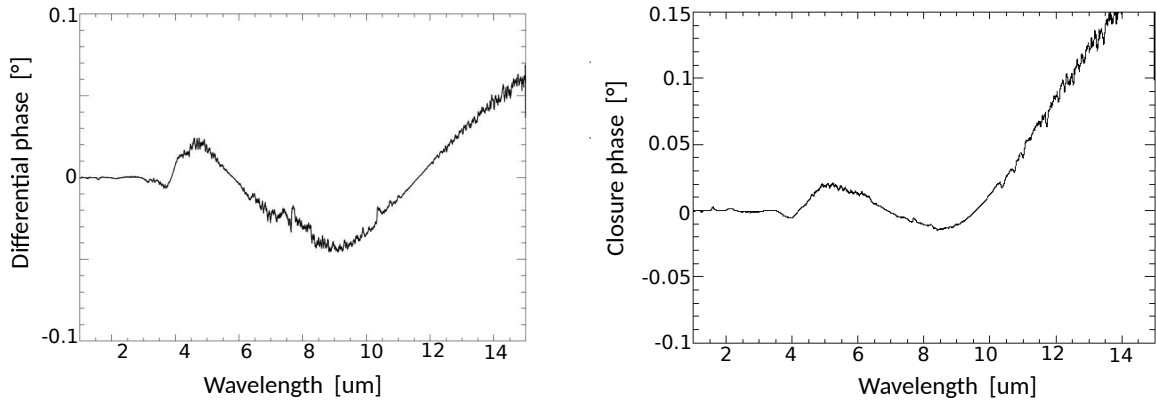


Figure 4. Left panel: Expected differential phase signal produced by Gliese 86b between 1 μm and 15 μm , with a mean projected baseline of about 110 m. Right panel: Expected closure phase signal between 1 μm and 15 μm , with the UT1-UT3-UT4 triplet.

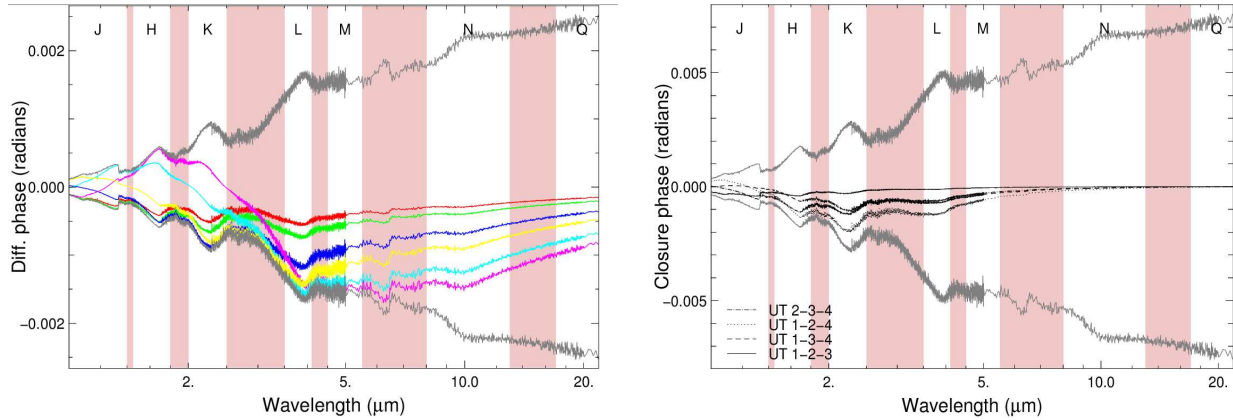


Figure 5. Expected differential phases (left) and closure phases (right) for τ Boo b with MATISSE (L/M and N bands).

According to Figs. 4 and 5, one would need a typical accuracy on closure phases and/or differential phases better than 10^{-3} rad ($\sim 0.05^\circ$). From considerations of the fundamental noises only (no systematics), the L band should be the most advantageous wavelength for exoplanets observations. Preliminary estimates of the fundamental error on the MATISSE phase measurements indicates that an accuracy of 10^{-3} rad would be achievable in about 10 hours of observation. These estimates will be refined as the instrument will be fully tested. The exoplanet science case is thus very challenging for MATISSE. To reach the necessary accuracies, the most critical aspect will be the fine correction of the instrumental phase and the 2nd order chromatic effects due to the atmospheric water vapor.^{58,59}

To graduate the difficulty and get the complete properties and biases characteristics of the MATISSE instrument at high dynamic range, it is foreseen to observe first single-lined high-contrast binaries and possibly binary brown dwarves.

4.2 Solar system minor bodies

Information about the physical properties of asteroids and comets, such as sizes, albedos, masses, composition and surface characteristics, provides essential constraints to models of the formation and collisional evolution of these bodies.⁶⁰⁻⁶² In turn, the properties and the history of minor bodies provide constrains to the processes

that led to the formation and the evolution of the terrestrial planets in our Solar System. Moreover, asteroids are involved in understanding other key issues in Solar System science, such as the delivery of water and organic molecules to Earth, the danger represented by Near Earth Objects and its mitigation,⁶³ the role of impacts in affecting Earth's climate and mass extinction events. Despite the fact that more than 720.000 asteroids are catalogued today, crucial parameters, such as composition and density, are known only for a few bodies. When compared with the densities of meteorites – a partial sample of the building blocks of asteroids that survive the passage through the Earth's atmosphere – one can deduce the bulk densities of these bodies. The latter parameter is directly related to the nature of asteroid interiors (e.g. fragmented, monolithic, differentiated).⁶⁴

The VLTI can spatially resolve asteroids in a range of sizes and heliocentric distances that are not accessible to other techniques such as adaptive optics and radar mapping. With temperatures ranging from 200-250 K in the Main Belt to 400-450 K in the near-Earth space, the asteroid emission peaks between 7 and 14 μm .⁶⁵ The MIR domain is thus particularly well suited for the observation of asteroids. The feasibility of MIR interferometric observations of asteroids has been demonstrated with VLTI/MIDI for some Main-Belt Asteroids (MBAs). This leads to characterisation of their physical properties such as size and shape,⁶⁶ thermal inertia^{67,68} or internal structure.⁶⁹ With the use of four telescopes and an extended spectral coverage down to 3 μm , MATISSE will allow to go further in the physical characterisation of asteroids and comets. Figure 6 shows that with a limiting flux of 1 Jy in N band, a few hundreds of asteroids become observable with MATISSE.

In the following, two exemplary science cases where MATISSE could provide new and decisive constraints are described:

Binary asteroids A fundamental contribution of MATISSE to the physical characterisation of small bodies will be the determination of the separation of the components, mutual orbital parameters, sizes and shapes of asteroids with satellites. This is by far the most productive method to determine asteroid densities and, in principle, not biased towards large objects. This method can provide accurate masses of asteroids since the orbital period and semimajor axis of the satellite uniquely determine the mass of the system. The best observations yield errors of only a few percent in mass.

Asteroids with satellites have now been found in every major dynamical group: near-Earth asteroids (NEAs), MBAs, Jupiter Trojans, Centaurs and Trans-Neptunian objects (TNOs). Statistical studies of the occurrence of asteroid satellites indicate that 15% of the asteroids with size < 20km have a satellite. Up to now, kilometer-sized binary asteroids have been studied essentially by radar⁷⁰ and by the photometric observation of mutual eclipses. However, radar is limited to NEAs during favourably close approaches with Earth since the signal-to-noise ratio of radar observations scales with r^{-4} , where r is the asteroid-radar distance. In the other dynamical populations, binaries have been discovered through direct imaging using adaptive optics on 8 and 10m class telescopes (VLT, Keck) or using the HST (with its superior resolution in space). However, this technique is limited to well-separated (>100 mas) binaries involving large (>100 km) bodies. Several of these large bodies have been characterised.⁷¹⁻⁷⁷ These objects show a remarkable range of orbital and physical characteristics: orbital periods between 0.5 to 80 days, secondary-to-primary size ratios between 0.1 and 1, and an asteroid bulk density between 0.7 and 3.5 g cm^{-3} , which highlight the potential of the study of binary asteroids for the analysis of their internal structure.

MATISSE will allow targeting the population of binaries discovered by means of photometric lightcurves. These systems are typically too small to be characterised with direct imaging and too distant for radar. High-angular-resolution observations (<100 mas) are thus critical for the characterisation of small and distant binaries in the Main Belt. The challenge that can be overcome by MATISSE is to determine the semimajor axis of the system. In general this requires spatially resolving the secondary from the primary. In principle, the density of these bodies can be derived from extensive lightcurve observations over a large range of solar phase angles and several epochs. However, severe difficulties arise in the case of MBAs, which are observable over a relatively moderate range of phase angle.⁷⁸ The orbital period, however, can be derived accurately by timing of the mutual eclipses.

By combining optical lightcurves and interferometric measurements, we will thus be able to derive full sets of orbital parameters for these systems, including system mass and provide more accurate density estimates. The latter will be derived from the additional knowledge of the size and shape of the primary component, which we

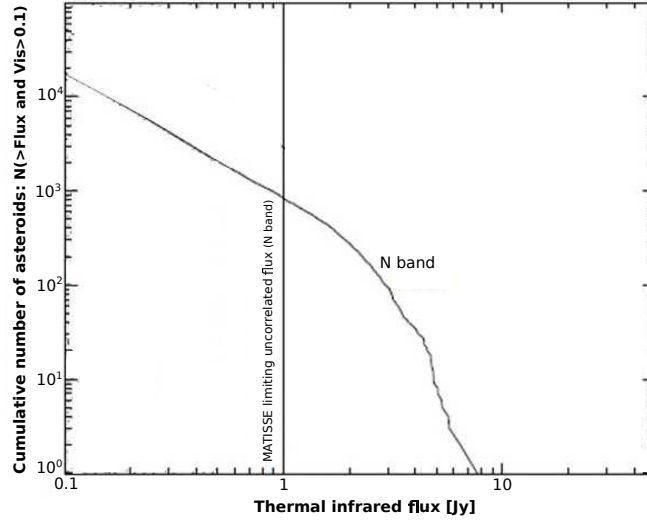


Figure 6. Cumulative number of Main-Belt asteroids observable with the VLTI in N band as function of their N band flux (visibility > 0.1). Diameters of asteroids are calculated from the known absolute magnitudes and assuming a geometric visible albedo of 0.11. The visibility is calculated assuming a uniform disk and a baseline of 24 m. A vertical line is drawn in correspondence with the sensitivity goal of MATISSE in the N band of 1 Jy (uncorrelated flux).

will derive directly from the visibility, as done in previous studies.^{66,69} A larger program based on this approach can produce asteroid density estimates for bodies in a range of sizes and heliocentric distances that cannot be reached by other means. MATISSE will provide simultaneous observations with four different baselines, leading to six simultaneous visibility points. In the case of binary asteroid studies, this will lead to a much better constraint on the angular separation of the system, and will allow us to determine, in one single observation, the 'true' angular separation as projected onto the plane of the sky (and not only along the baseline direction).

As already shown,⁶⁹ this work will be based on the combination of constraints obtained from optical lightcurves (orbital period, pole orientation, orbital phase) with interferometric measurements of the size and separation of binary components. Such measurement will be performed through model fitting of visibilities using geometrical models. UTs are preferable given the low brightness of the photometric binary targets. The binarity signature in the visibilities will be detectable only if the coherent flux contribution from the secondary component will be higher than the fundamental noises level. High sensitivity in correlated flux will thus be a key element in this study. Both absolute and relative measures will be important for these studies. On one hand, good accuracy on absolute visibility levels will be important to estimate the individual size of the binary components. On the other hand, accuracy on relative measures (i.e., differential visibility) will be a key element to distinguish binarity signature in the visibilities and measure the separation of the components.

Surface properties of asteroids Concerning the study of asteroid surface properties, MIDI was already used to derive the value of asteroid thermal inertias.^{67,68} The latter is the resistance of a material to temperature change and is a sensitive indicator for the properties of the grainy soil⁶⁵ on asteroids. Thermal inertia (Γ) is defined as $\Gamma = \sqrt{\kappa\rho C}$, where κ is the material's thermal conductivity, ρ is its density, and C is its heat capacity. MATISSE data will be sensitive to the surface temperature distribution, which is strongly affected by the value of the thermal inertia.^{65,79}

The availability of L & M bands for MATISSE will allow us to constrain the spatial distribution of water ice and hydrated minerals on the surface of asteroids. This enables us to shed light on the way water has been incorporated and processed through aqueous alteration on the surface of asteroids e.g. by impacts (the water feature is spatially localised on the surface) or by accretion of water/ice rich pebbles (the water feature is evenly distributed over the surface). MATISSE can be used to obtain interferometric observations of asteroids that present hydration and water ice absorption features at $\sim 3 \mu\text{m}$. In particular, one can observe asteroids known to present absorption features due to OH vibrational fundamentals ($\sim 2.75 \mu\text{m}$), for Ceres, Pallas and Hygiea,

or due to the first overtone of H₂O ($\sim 3.1 \mu\text{m}$). A possible approach will be to measure and to compare the correlated fluxes, visibilities, and closure phases in the $3 \mu\text{m}$ absorption feature with the ones obtained in the L band continuum which traces the global angular size of the asteroid and possibly sub-structures. As the asteroids will rotate significantly during one single night, one can map the spatial distribution of water ice and hydrated minerals on their surface. In parallel, the N band data can be used to constrain further the surface temperature distribution of these asteroids, and especially their thermal inertia, as successfully done in the past by using MIDI.^{67,68}

5. ACTIVE GALACTIC NUCLEI

The spectacular angular resolution offered by MATISSE will also provide us with a unique opportunity to study AGNs. The innermost dust distribution in AGNs (the putative *torus*) is most likely responsible for the viewing-angle-dependent obscuration of the central engine. Therefore, high spatial resolution studies of the inner dust distribution in AGNs are essential for improving our understanding of AGN unification schemes. Furthermore, the high spectral resolution of 5000 of MATISSE can be used to study the kinematics of the Broad Line Region (BLR).

Previous infrared interferometric observations have shown that the structure of the dust distribution is much more complicated than predicted by classical torus models, because a large amount of dust along the polar direction was discovered in many objects. Therefore, interferometric studies can provide crucial constraints for the innermost mas-scale dust structures in AGNs and help us to shape a new picture of AGN unification.

Previous VLTI studies of AGNs in the near- and mid-infrared were challenging for several reasons: (1) The limiting magnitude of AMBER observations of about $K \sim 9\text{--}10$; (2) the limiting H band magnitude of the fringe tracker FINITO of $H \sim 6\text{--}8$; and (3) the two-telescope beam combination of the mid-infrared MIDI instrument, which did not allow us to measure closure phases. In contrast to MIDI, MATISSE will be able to perform aperture-synthesis imaging of AGNs in the L, M, and N bands.

Important objects for MATISSE observations are NGC 1068, the Circinus AGN, Cen A, the nearest QSO 3C273, and also many fainter objects. Below, we briefly summarize some of the results obtained already with infrared interferometric observations to illustrate the feasibility of MATISSE observations of AGNs. These results are also important for the planning of future imaging projects, as artificial substructures may appear in reconstructed images if, for example, the low spatial frequencies of very extended structures are under-sampled due to the lack of short baselines. In the following paragraphs, we briefly discuss some of the resolved object structures that will play an important role in MATISSE aperture-synthesis imaging.

NGC 1068. The dust distribution in NGC 1068 was resolved by near-infrared bispectrum speckle interferometry,^{80,81} near-infrared VLTI-VINCI interferometry,⁸² and mid-infrared (8 to $13 \mu\text{m}$) VLTI-MIDI interferometry.^{83,84} The bispectrum speckle interferometry K band image shows a compact, elongated dust distribution with a FWHM Gaussian fit diameter of $\sim 18 \times 39 \text{ mas}$ or $1.3 \times 2.8 \text{ pc}$. This structure is extended to the north-west along a position angle of approximately -16° (the H band image has a similar structure). The additionally resolved extended northern component (PA $\sim 0^\circ$) has a length of about 400 mas or 29 pc. Mid-infrared MIDI observations⁸³ resolved a warm $\sim 2.1 \times 3.4 \text{ pc}$ structure surrounding a compact ($\sim 0.7 \text{ pc}$) hot component. Additional MIDI observations⁸⁴ with short baselines allowed a more detailed modeling of the intensity distribution.

Circinus. To interpret the large number of obtained mid-infrared MIDI correlated flux spectra and wavelength-differential phases, models consisting of several black-body emitters with a Gaussian brightness distribution and with dust extinction were used.^{85,86} The modeling of all interferometric data reveals that the mid-infrared emission can be explained by three distinct components: A compact, highly inclined (almost edge-on) disk-like component, a compact circular component, and an extended dust structure elongated in polar direction. The disk-like component has a Gaussian FWHM of $\sim 7 \times 35 \text{ mas}$ ($\sim 0.14 \times 0.70 \text{ pc}$) and is elongated along a PA of $\sim 44^\circ$, that is almost identical to the PA of the edge-on H₂O megamaser disk (PA $\sim 44^\circ$) and approximately perpendicular to the PA of the ionization cone (PA $\sim 314^\circ$) and the radio lobes (PA ~ 115 and 295°). The extended component has a size of $\sim 50 \times 80 \text{ mas}$ ($\sim 1.0 \times 1.6 \text{ pc}$) and is responsible for 80% of the mid-infrared emission. It is elongated along a PA $\sim 310^\circ$. The derived three-component structure of the dust distribution shows that the dust distribution is more complicated than expected from axisymmetric torus models.

Cen A. At a distance of only 3.8 Mpc, Centaurus A (NGC 5128) is the nearest radio-loud AGN. VLTI/MIDI measurements^{87,88} allowed the resolution of the nuclear mid-infrared emission and constrain parameters of the emission components. The MIDI observations can be explained by a two-component model of an unresolved synchrotron point source (diameter ≤ 7 mas) and an extended dust emission component. The extended component is elongated with a size of about 1.3×0.5 pc.⁸⁷

NGC 3783 AMBER observations in the near- and mid-infrared. A K band torus radius of ~ 0.74 mas or 0.16 pc was derived from the obtained AMBER visibilities.⁸⁹ Temperature-density gradient models were used to interpret the K band AMBER observations, mid-infrared MIDI observations, and the SED. The results show that an inner hot model component with a temperature of 1400 K and a radius of ~ 0.16 pc are required in addition to a more extended component in order to explain all observations. This hot component might play a similar role as the puffed-up inner rim discovered in several young stellar objects near the dust sublimation radius.

MIDI Large Programme. The *MIDI Large AGN Programme* studied the correlated and total fluxes of 23 AGNs and derived flux and size estimates at $12 \mu\text{m}$ using simple geometric models.⁹⁰ For 18 of the sources, two different nuclear components can be distinguished in the radial plot fits (with different relative flux contributions from the compact and extended components). The different two-component structures probably cause the large scatter of the derived size-luminosity relation.

AMBER observations of the quasar 3C273 with spectral resolution of 1500. AMBER observations of the nearest QSO 3C273 ($K=10$)⁹¹ with spectral resolution of 1500 provided, for the first time, spectrally resolved AGN observations in many spectral channels distributed across the Paschen α line. From the interferograms wavelength-differential phases were derived, which can be used to study the kinematics of the BLR.

Various torus models have been developed, for example, models with a homogeneous, gravitationally settled dust distribution, clumpy models, and hydrodynamical models.^{92–96} MATISSE aperture-synthesis imaging of the nearest AGNs will probably be able to discriminate between these models and constrain model parameters. The observed two-component structure of the dust distribution clearly demonstrates that the dust distribution is more complicated than has been predicted by classical models. Notably, in several objects, large amounts of dust was discovered along the polar direction. This unexpected complexity clearly requires aperture-synthesis imaging to get a realistic insight in the unknown structure of the dust distribution. Therefore, MATISSE can provide crucial constraints for the innermost dust structures in AGNs. These observations are essential for updating our understanding of AGN unification schemes. Furthermore, high spatial and high spectral resolution interferometric observations will provide a exiting new opportunity to improve our understanding of the kinematics of the AGN BLR.

6. SUMMARY

We have presented a selection of science cases for MATISSE, the 2nd generation mid-infrared spectro-interferometer for the Very Large Telescope Interferometer. While this list of science cases is by no means comprehensive, it demonstrates the instrument’s great potential for discoveries in a broad range of astrophysical topics.

Moreover, while MATISSE will provide the basis for the reconstruction of high-angular resolution images in the mid-infrared wavelength range, we have demonstrated that even the direct analysis of the observational data through model fitting will provide far more constraints than it was possible with its predecessor MIDI. Furthermore, taking into account the various spectroscopic modes as well as the multi-wavelength aspect, MATISSE has been shown to provide unique insight into the nature of various astrophysical sources, complementary to those that can be derived with long-baseline interferometers and other currently or soon available high angular resolution instruments, operating in the near-infrared and submillimeter/millimeter wavelength range.

ACKNOWLEDGMENTS

SW acknowledges funding through the DFG grant WO 857/13-1.

REFERENCES

- [1] B. Lopez, S. Lagarde, W. Jaffe, R. Petrov, M. Schöller, P. Antonelli, U. Beckmann, P. Berio, F. Bettonvil, A. Glindemann, J. C. Gonzalez, U. Graser, K. H. Hofmann, F. Millour, S. Robbe-Dubois, L. Venema, S. Wolf, T. Henning, T. Lanz, G. Weigelt, T. Agocs, C. Bailet, Y. Bresson, P. Bristow, M. Dugué, M. Heininger, G. Kroes, W. Laun, M. Lehmitz, U. Neumann, J.-C. Augereau, G. Avila, J. Behrend, G. van Belle, J.-P. Berger, R. van Boekel, S. Bonhomme, P. Bourget, R. Brast, J. M. Clause, C. Connot, R. Conzelmann, P. Cruzalèbes, G. Csepány, W. Danchi, M. Delbo, F. Delplancke, C. Dominik, A. van Duin, E. Elswijk, Y. Fantei, G. Finger, A. Gabasch, J. Gay, P. Girard, V. Girault, P. Gitton, A. Glazenberg, F. Gonte, F. Guitton, S. Guniat, M. De Haan, P. Haguenaer, H. Hanenburg, M. Hogerheijde, R. ter Horst, J. Hron, Y. Hugues, C. Hummel, J. Idserda, D. Ives, G. Jakob, A. Jasko, P. Jolley, S. Kiraly, R. Köhler, J. Kragt, T. Kroener, S. Kuindersma, L. Labadie, C. Leinert, R. le Poole, J.-L. Lizon, C. Lucuix, A. Marcotto, F. Martinache, G. Martinot-Lagarde, R. Mathar, A. Matter, N. Mauclet, L. Mehrgan, A. Meilland, K. Meisenheimer, J. Meisner, M. Mellein, S. Menardi, J. L. Menut, A. Mérand, S. Morel, L. Mosoni, R. Navarro, E. Nussbaum, S. Ottogalli, R. Palsa, J. Panduro, E. Pantin, T. Parra, I. Percheron, T. P. Duc, J.-U. Pott, E. Pozna, F. Przygodda, Y. Rabbia, A. Richichi, F. Rigal, R. Roelfsema, G. Rupprecht, D. Schertl, C. Schmidt, N. Schuhler, M. Schuil, A. Spang, J. Stegmeier, L. Thiam, N. Tromp, F. Vakili, M. Vannier, K. Wagner, and J. Woillez, “An Overview of the MATISSE Instrument — Science, Concept and Current Status,” *The Messenger* **157**, 5–12 (2014).
- [2] S. Wolf, F. Malbet, R. Alexander, J.-P. Berger, M. Creech-Eakman, G. Duchêne, A. Dutrey, C. Mordasini, E. Pantin, F. Pont, J.-U. Pott, E. Tatulli, and L. Testi, “Circumstellar disks and planets. Science cases for next-generation optical/infrared long-baseline interferometers,” *A&A Rev.* **20**, 52 (2012).
- [3] C. J. Lada, “Star formation - From OB associations to protostars,” in *IN: Star forming regions; Proceedings of the Symposium*, 1–17, Seward Observatory, Tucson, AZ (1987).
- [4] J. P. Williams and L. A. Cieza, “Protoplanetary Disks and Their Evolution,” *Annual Review of Astronomy and Astrophysics* **49**, 67–117 (2011).
- [5] D. Fedele, M. E. Van Den Ancker, T. Henning, R. Jayawardhana, and J. M. Oliveira, “Timescale of mass accretion in pre-main-sequence stars,” *Astronomy and Astrophysics* **510**, 72 (2010).
- [6] A. Natta, L. Testi, and S. Randich, “Accretion in the ρ -Ophiuchi pre-main sequence stars,” *Astronomy and Astrophysics* **452**, 245–252 (2006).
- [7] G. J. Herczeg and L. A. Hillenbrand, “UV Excess Measures of Accretion onto Young Very Low Mass Stars and Brown Dwarfs,” *The Astrophysical Journal* **681**, 594–625 (2008).
- [8] M. Fang, J. S. Kim, R. van Boekel, A. Sicilia-Aguilar, T. Henning, and K. Flaherty, “Young Stellar Objects in Lynds 1641: Disks, Accretion, and Star Formation History,” *The Astrophysical Journal Supplement* **207**, 5 (2013).
- [9] P. Bodenheimer and J. B. Pollack, “Calculations of the accretion and evolution of giant planets The effects of solid cores,” *Icarus (ISSN 0019-1035)* **67**, 391–408 (1986).
- [10] D. J. Wilner, T. L. Bourke, C. M. Wright, J. K. Jorgensen, E. F. Van Dishoeck, and T. Wong, “Disks around the Young Stars TW Hydrae and HD 100546 Imaged at 3.4 Millimeters with the Australia Telescope Compact Array,” *The Astrophysical Journal* **596**, 597–602 (2003).
- [11] C. A. Grady, G. Schneider, K. Hamaguchi, M. L. Sitko, W. J. Carpenter, D. Hines, K. A. Collins, G. M. Williger, B. E. Woodgate, T. Henning, F. Ménard, D. Wilner, R. Petre, P. Palunas, A. Quirrenbach, J. A. I. Nuth, M. D. Silverstone, and J. S. Kim, “The Disk and Environment of a Young Vega Analog: HD 169142,” *The Astrophysical Journal* **665**, 1391–1406 (2007).
- [12] J. H. Debes, H. Jang-Condell, A. J. Weinberger, A. Roberge, and G. Schneider, “The 0.5-2.22 μm Scattered Light Spectrum of the Disk around TW Hya: Detection of a Partially Filled Disk Gap at 80 AU,” *The Astrophysical Journal* **771**, 45 (2013).
- [13] C. Doucet, E. Habart, E. Pantin, C. Dullemond, P.-O. Lagage, C. Pinte, G. Duchêne, and F. Ménard, “HD 97048: a closer look at the disk,” *Astronomy and Astrophysics* **470**, 625–631 (2007).

- [14] A. Partnership, C. L. Brogan, L. M. Pérez, T. R. Hunter, W. R. F. Dent, A. Hales, R. E. Hills, S. Corder, E. B. Fomalont, C. Vlahakis, Y. Asaki, D. Barkats, A. Hirota, J. A. Hodge, C. M. V. Impellizzeri, R. Kneissl, E. Liuzzo, R. Lucas, N. Marcelino, S. Matsushita, K. Nakanishi, N. Phillips, A. M. S. Richards, I. Toledo, R. Aladro, D. Brogiere, J. R. Cortes, P. C. Cortes, D. Espada, F. Galarza, D. Garcia-Appadoo, L. Guzman-Ramirez, E. M. Humphreys, T. Jung, S. Kamenno, R. A. Laing, S. Leon, G. Marconi, A. Mignano, B. Nikolic, L. Å. Nyman, M. Radiszcz, A. Remijan, J. A. Rodon, T. Sawada, S. Takahashi, R. P. J. Tilanus, B. Vila Vilaro, L. C. Watson, T. Wiklind, E. Akiyama, E. Chapillon, I. de Gregorio-Monsalvo, J. Di Francesco, F. Gueth, A. Kawamura, C. F. Lee, Q. Nguyen Luong, J. Mangum, V. Piétu, P. Sanhueza, K. Saigo, S. Takakuwa, C. Ubach, T. Van Kempen, A. Wootten, A. Castro-Carrizo, H. Francke, J. Gallardo, J. Garcia, S. Gonzalez, T. Hill, T. Kaminski, Y. Kurono, H. Y. Liu, C. López, F. Morales, K. Plarre, G. Schieven, L. Testi, L. Videla, E. Villard, P. Andreani, J. E. Hibbard, and K. Tatematsu, “The 2014 ALMA Long Baseline Campaign: First Results from High Angular Resolution Observations toward the HL Tau Region,” *The Astrophysical Journal Letters* **808**, L3 (2015).
- [15] S. M. Andrews, D. J. Wilner, Z. Zhu, T. Birnstiel, J. M. Carpenter, L. M. Pérez, X.-n. Bai, K. I. Öberg, A. M. Hughes, A. Isella, and L. Ricci, “Ringed Substructure and a Gap at 1 AU in the Nearest Protoplanetary Disk,” *arXiv.org*, arXiv:1603.09352 (2016).
- [16] C. Carrasco-Gonzalez, T. Henning, C. J. Chandler, H. Linz, L. Perez, L. F. Rodriguez, R. Galvan-Madrid, G. Anglada, T. Birnstiel, R. van Boekel, M. Flock, H. Klahr, E. Macias, K. Menten, M. Osorio, L. Testi, J. M. Torrelles, and Z. Zhu, “The VLA view of the HL Tau Disk - Disk Mass, Grain Evolution, and Early Planet Formation,” *ArXiv e-prints* (2016).
- [17] E. Akiyama, T. Muto, N. Kusakabe, A. Kataoka, J. Hashimoto, T. Tsukagoshi, J. Kwon, T. Kudo, R. Kandori, C. A. Grady, M. Takami, M. Janson, M. Kuzuhara, T. Henning, M. L. Sitko, J. C. Carson, S. Mayama, T. Currie, C. Thalmann, J. Wisniewski, M. Momose, N. Ohashi, L. Abe, W. Brandner, T. D. Brandt, S. Egener, M. Feldt, M. Goto, O. Guyon, Y. Hayano, M. Hayashi, S. Hayashi, K. W. Hodapp, M. Ishi, M. Iye, G. R. Knapp, T. Matsuo, M. W. McElwain, S. Miyama, J. I. Morino, A. Moro-Martin, T. Nishimura, T. S. Pyo, G. Serabyn, T. Suenaga, H. Suto, R. Suzuki, Y. H. Takahashi, N. Takato, H. Terada, D. Tomono, E. L. Turner, M. Watanabe, T. Yamada, H. Takami, T. Usuda, and M. Tamura, “Discovery of a Disk Gap Candidate at 20 AU in TW Hydrae,” *The Astrophysical Journal Letters* **802**, L17 (2015).
- [18] V. A. Rapson, J. H. Kastner, M. A. Millar-Blanchaer, and R. Dong, “Peering into the Giant-planet-forming Region of the TW Hydrae Disk with the Gemini Planet Imager,” *The Astrophysical Journal Letters* **815**, L26 (2015).
- [19] M. Benisty, A. Juhasz, A. Boccaletti, H. Avenhaus, J. Milli, C. Thalmann, C. Dominik, P. Pinilla, E. Buenzli, A. Pohl, J. L. Beuzit, T. Birnstiel, J. de Boer, M. Bonnefoy, G. Chauvin, V. Christiaens, A. Garufi, C. Grady, T. Henning, N. Huélamo, A. Isella, M. Langlois, F. Ménard, D. Mouillet, J. Olofsson, E. Pantin, C. Pinte, and L. Pueyo, “Asymmetric features in the protoplanetary disk MWC 758,” *Astronomy and Astrophysics* **578**, L6 (2015).
- [20] T. Stolker, C. Dominik, H. Avenhaus, M. Min, J. de Boer, C. Ginski, H. M. Schmid, A. Juhasz, A. Bazzon, L. B. F. M. Waters, A. Garufi, J.-C. Augereau, M. Benisty, A. Boccaletti, T. Henning, A. L. Maire, F. Ménard, M. R. Meyer, M. Langlois, C. Pinte, S. P. Quanz, C. Thalmann, J. L. Beuzit, M. Carbillet, A. Costille, K. Dohlen, M. Feldt, D. Gisler, D. Mouillet, A. Pavlov, D. Perret, C. Petit, J. Pragt, S. Rochat, R. Roelfsema, B. Salasnich, C. Soenke, and F. Wildi, “Shadows cast on the transition disk of HD 135344B,” *arXiv.org*, arXiv:1603.00481 (2016).
- [21] L. Chen, A. Kreplin, Y. Wang, G. Weigelt, K. H. Hofmann, S. Kraus, D. Schertl, S. Lagarde, A. Natta, R. Petrov, S. Robbe-Dubois, and E. Tatulli, “Near-infrared interferometric observation of the Herbig Ae star HD 144432 with VLTI/AMBER,” *Astronomy and Astrophysics* **541**, A104 (2012).
- [22] A. A. Schegerer, T. Ratzka, P. A. Schuller, S. Wolf, L. Mosoni, and C. Leinert, “Multiwavelength interferometric observations and modeling of circumstellar disks,” *Astronomy and Astrophysics* **555**, 103 (2013).
- [23] A. Matter, L. Labadie, A. Kreplin, B. Lopez, S. Wolf, G. Weigelt, S. Ertel, J.-U. Pott, and W. C. Danchi, “Evidence of a discontinuous disk structure around the Herbig Ae star HD 139614,” *Astronomy and Astrophysics* **561**, 26 (2014).

- [24] C. Leinert, U. Graser, L. B. Waters, G. Perrin, B. Lopez, V. Coudé du Foresto, A. W. Glazenberg-Kluttig, J. C. de Haas, T. M. Herbst, W. Jaffe, P. J. Lena, R. Lenzen, R. S. le Poole, S. Ligorì, R. Mundt, J.-W. Pel, I. L. Porro, and O. von der Luehe, “10-um interferometry on the VLTI with the MIDI instrument: a preview,” *Proc. SPIE Vol. 4006* **4006**, 43–53 (2000).
- [25] C. Leinert, R. van Boekel, L. B. F. M. Waters, O. Chesneau, F. Malbet, R. Köhler, W. Jaffe, T. Ratzka, A. Dutrey, T. Preibisch, U. Graser, E. Bakker, G. Chagnon, W. D. Cotton, C. Dominik, C. P. Dullemond, A. W. Glazenberg-Kluttig, A. Glindemann, T. Henning, K. H. Hofmann, J. de Jong, R. Lenzen, S. Ligorì, B. Lopez, J. Meisner, S. Morel, F. Paresce, J. W. Pel, I. Percheron, G. Perrin, F. Przygodda, A. Richichi, M. Schöller, P. Schuller, B. Stecklum, M. E. Van Den Ancker, O. von der Luehe, and G. Weigelt, “Mid-infrared sizes of circumstellar disks around Herbig Ae/Be stars measured with MIDI on the VLTI,” *Astronomy and Astrophysics* **423**, 537–548 (2004).
- [26] R. van Boekel, M. Min, C. Leinert, L. B. F. M. Waters, A. Richichi, O. Chesneau, C. Dominik, W. Jaffe, A. Dutrey, U. Graser, T. Henning, J. de Jong, R. Köhler, A. De Koter, B. Lopez, F. Malbet, S. Morel, F. Paresce, G. Perrin, T. Preibisch, F. Przygodda, M. Schöller, and M. Wittkowski, “The building blocks of planets within the ‘terrestrial’ region of protoplanetary disks,” *Nature* **432**, 479–482 (2004).
- [27] A. A. Schegerer, S. Wolf, T. Ratzka, and C. Leinert, “The T Tauri star RY Tauri as a case study of the inner regions of circumstellar dust disks,” *Astronomy and Astrophysics* **478**, 779 (2008).
- [28] G. D. Mulders, S.-J. Paardekooper, O. Panić, C. Dominik, R. van Boekel, and T. Ratzka, “Planet or brown dwarf? Inferring the companion mass in HD 100546 from the wall shape using mid-infrared interferometry,” *Astronomy and Astrophysics* **557**, 68 (2013).
- [29] J. Menu, R. van Boekel, T. Henning, C. J. Chandler, H. Linz, M. Benisty, S. Lacour, M. Min, C. Waelkens, S. M. Andrews, N. Calvet, J. M. Carpenter, S. A. Corder, A. T. Deller, J. S. Greaves, R. J. Harris, A. Isella, W. Kwon, J. Lazio, J. B. Le Bouquin, F. Ménard, L. G. Mundy, L. M. Pérez, L. Ricci, A. I. Sargent, S. Storm, L. Testi, and D. J. Wilner, “On the structure of the transition disk around TW Hydrae,” *Astronomy and Astrophysics* **564**, A93 (2014).
- [30] J. Menu, R. van Boekel, T. Henning, C. Leinert, C. Waelkens, and L. B. F. M. Waters, “The structure of disks around intermediate-mass young stars from mid-infrared interferometry. Evidence for a population of group II disks with gaps,” *Astronomy and Astrophysics* **581**, A107 (2015).
- [31] G. Meeus, L. B. F. M. Waters, J. Bouwman, M. E. Van Den Ancker, C. Waelkens, and K. Malfait, “ISO spectroscopy of circumstellar dust in 14 Herbig Ae/Be systems: Towards an understanding of dust processing,” *Astronomy and Astrophysics* **365**, 476–490 (2001).
- [32] B. R. Brandl, R. Lenzen, E. Pantin, A. Glasse, J. Blommaert, L. Venema, F. J. Molster, R. Siebenmorgen, S. Kendrew, M. Baes, H. Böhnhardt, W. Brandner, E. van Dishoeck, T. Henning, H. U. Käufl, P.-O. Lagage, T. J. T. Moore, C. Waelkens, and P. van der Werf, “Instrument concept and science case for the mid-IR E-ELT imager and spectrograph METIS,” in *Proceedings of the SPIE*, 77352G, Leiden Observatory, Leiden Univ., Netherlands (2010).
- [33] S. Kraus, K.-H. Hofmann, M. Benisty, J.-P. Berger, O. Chesneau, A. Isella, F. Malbet, A. Meilland, N. Nardetto, A. Natta, T. Preibisch, D. Schertl, M. Smith, P. Stee, E. Tatulli, L. Testi, and G. Weigelt, “The origin of hydrogen line emission for five Herbig Ae/Be stars spatially resolved by VLTI/AMBER spectro-interferometry,” *Astronomy & Astrophysics* **489**, 1157–1173 (2008).
- [34] G. Weigelt, V. P. Grinin, J. H. Groh, K.-H. Hofmann, S. Kraus, A. S. Miroshnichenko, D. Schertl, L. V. Tambovtseva, M. Benisty, T. Driebe, S. Lagarde, F. Malbet, A. Meilland, R. Petrov, and E. Tatulli, “VLTI/AMBER spectro-interferometry of the Herbig Be star MWC 297 with spectral resolution 12 000,” *Astronomy & Astrophysics* **527**, A103 (2011).
- [35] A. Caratti o Garatti, L. V. Tambovtseva, R. Garcia Lopez, S. Kraus, D. Schertl, V. P. Grinin, G. Weigelt, K.-H. Hofmann, F. Massi, S. Lagarde, M. Vannier, and F. Malbet, “AMBER/VLTI high spectral resolution observations of the Br γ emitting region in HD 98922. A compact disc wind launched from the inner disc region,” *Astronomy & Astrophysics* **582**, A44 (2015).
- [36] R. Garcia Lopez, L. V. Tambovtseva, D. Schertl, V. P. Grinin, K.-H. Hofmann, G. Weigelt, and A. Caratti o Garatti, “Probing the accretion-ejection connection with VLTI/AMBER. High spectral resolution observations of the Herbig Ae star HD 163296,” *Astronomy & Astrophysics* **576**, A84 (2015).

- [37] S. D. Brittain, T. W. Rettig, T. Simon, C. Kulesa, M. A. DiSanti, and N. Dello Russo, “CO Emission from Disks around AB Aurigae and HD 141569: Implications for Disk Structure and Planet Formation Timescales,” *The Astrophysical Journal* **588**, 535–544 (2003).
- [38] G. A. Blake and A. C. A. Boogert, “High-Resolution 4.7 Micron Keck/NIRSPEC Spectroscopy of the CO Emission from the Disks Surrounding Herbig Ae Stars,” *The Astrophysical Journal Letters* **606**, L73–L76 (2004).
- [39] T. W. Rettig, J. Haywood, T. Simon, S. D. Brittain, and E. Gibb, “Discovery of CO Gas in the Inner Disk of TW Hydrae,” *The Astrophysical Journal Letters* **616**, L163–L166 (2004).
- [40] C. Salyk, G. A. Blake, A. C. A. Boogert, and J. M. Brown, “Molecular Gas in the Inner 1 AU of the TW Hya and GM Aur Transitional Disks,” *The Astrophysical Journal Letters* **655**, L105–L108 (2007).
- [41] C. Salyk, G. A. Blake, A. C. A. Boogert, and J. M. Brown, “CO Rovibrational Emission as a Probe of Inner Disk Structure,” *The Astrophysical Journal* **743**, 112 (2011).
- [42] K. M. Pontoppidan, G. A. Blake, and A. Smette, “The Structure and Dynamics of Molecular Gas in Planet-forming Zones: A CRIRES Spectro-astrometric Survey,” *The Astrophysical Journal* **733**, 84 (2011).
- [43] F. Kerschbaum, R. F. Wing, and J. Hron, Eds., *Why Galaxies Care about AGB Stars III: A Closer Look in Space and Time, Astronomical Society of the Pacific Conference Series* **497** (2015).
- [44] J. Walsh, E. Humphreys, and M. Wittkowski, “Report on the ESO Workshop ”Stellar End Products: The Low-mass - High-mass Connection”,” *The Messenger* **161**, 43–48 (2015).
- [45] P. Kervella, A. Mérand, G. Perrin, and V. Coudé du Foresto, “Extended envelopes around Galactic Cepheids. I. Carinae from near and mid-infrared interferometry with the VLTI,” *A&A* **448**, 623–631 (2006).
- [46] A. Mérand, P. Kervella, V. Coudé du Foresto, G. Perrin, S. T. Ridgway, J. P. Aufdenberg, T. A. ten Brummelaar, H. A. McAlister, L. Sturmann, J. Sturmann, N. H. Turner, and D. H. Berger, “Extended envelopes around Galactic Cepheids. II. Polaris and δ Cephei from near-infrared interferometry with CHARA/FLUOR,” *A&A* **453**, 155–162 (2006).
- [47] P. Kervella, A. Mérand, and A. Gallenne, “The circumstellar envelopes of the Cepheids Carinae and RS Puppis . Comparative study in the infrared with Spitzer, VLT/VISIR, and VLTI/MIDI,” *A&A* **498**, 425–443 (2009).
- [48] A. Gallenne, P. Kervella, and A. Mérand, “Thermal infrared properties of classical and type II Cepheids. Diffraction limited 10 μ m imaging with VLT/VISIR,” *A&A* **538**, A24 (2012).
- [49] A. Gallenne, A. Mérand, P. Kervella, O. Chesneau, J. Breitsfelder, and W. Gieren, “Extended envelopes around Galactic Cepheids. IV. T Monocerotis and X Sagittarii from mid-infrared interferometry with VLTI/MIDI,” *A&A* **558**, A140 (2013).
- [50] A. Gallenne, A. Mérand, P. Kervella, and J. H. V. Girard, “Spatially extended emission around the Cepheid RS Puppis in near-infrared hydrogen lines. Adaptive optics imaging with VLT/NACO,” *A&A* **527**, A51 (2011).
- [51] N. Nardetto, A. Stoekl, D. Bersier, and T. G. Barnes, “High-resolution spectroscopy for Cepheids distance determination. III. A relation between γ -velocities and γ -asymmetries,” *A&A* **489**, 1255–1262 (2008).
- [52] N. Nardetto, J. H. Groh, S. Kraus, F. Millour, and D. Gillet, “High-resolution spectroscopy for Cepheids distance determination. IV. Time series of H α line profiles,” *A&A* **489**, 1263–1269 (2008).
- [53] D. Segransan, J.-L. Beuzit, X. Delfosse, T. Forveille, M. Mayor, C. Perrier-Bellet, and F. Allard, “How AMBER will contribute to the search for brown dwarfs and extrasolar giant planets,” in *Interferometry in Optical Astronomy*, P. Léna and A. Quirrenbach, Eds., *SPIE proceedings* **4006**, 269–276 (2000).
- [54] B. Lopez, R. G. Petrov, and M. Vannier, “Direct detection of hot extrasolar planets with the VLTI using differential interferometry,” in *Interferometry in Optical Astronomy*, P. Léna and A. Quirrenbach, Eds., *SPIE proceedings* **4006**, 407–411 (2000).
- [55] M. Vannier, R. G. Petrov, B. Lopez, and F. Millour, “Colour-differential interferometry for the observation of extrasolar planets,” *Mon. Not. R. Astron. Soc.* **367**, 825–837 (2006).
- [56] D. Queloz, M. Mayor, L. Weber, A. Blécha, M. Burnet, B. Confino, D. Naef, F. Pepe, N. Santos, and S. Udry, “The CORALIE survey for southern extra-solar planets. I. A planet orbiting the star Gliese 86,” *Astron. Astrophys.* **354**, 99–102 (2000).

- [57] R. P. Butler, G. W. Marcy, E. Williams, H. Hauser, and P. Shirts, “Three New “51 Pegasi-Type” Planets,” *Astrophys. J. Lett.* **474**, L115–L118 (1997).
- [58] A. Matter, M. Vannier, S. Morel, B. Lopez, W. Jaffe, S. Lagarde, R. G. Petrov, and C. Leinert, “First step to detect an extrasolar planet using simultaneous observations with the VLTI instruments AMBER and MIDI,” *Astron. Astrophys.* **515**, A69 (2010).
- [59] R. N. Tubbs, J. A. Meisner, E. J. Bakker, and S. Albrecht, “Differential phase delay observations with VLTI-MIDI at N-band,” in *New Frontiers in Stellar Interferometry*, W. A. Traub, Ed., *SPIE proceedings* **5491**, 588 (2004).
- [60] A. Morbidelli, W. F. Bottke, D. Nesvorný, and H. F. Levison, “Asteroids were born big,” *Icarus* **204**, 558–573 (2009).
- [61] W. F. Bottke, M. Broz, D. P. O’Brien, A. Campo Bagatin, A. Morbidelli, and S. Marchi, “The Collisional Evolution of the Main Asteroid Belt,” in *Asteroids IV*, F. E. DeMeo and P. Michel, Eds., 1–24, University of Arizona Press (2015).
- [62] A. Johansen, E. Jaquet, J. N. Cuzzi, A. Morbidelli, and M. Gounelle, “New Paradigms For Asteroid Formation,” in *Asteroids IV*, 1–22 (2015).
- [63] A. Harris, M. Boslough, C. R. Chapman, L. Drube, and P. Michel, “Asteroid Impacts and Modern Civilization: Can we Prevent a Catastrophe?,” in *Asteroids IV*, University of Arizona Press, Tucson, AZ (2015).
- [64] G. Consolmagno, D. Britt, and R. Macke, “The significance of meteorite density and porosity,” *Chemie der Erde - Geochemistry* **68**, 1–29 (2008).
- [65] M. Delbo, M. Mueller, J. P. Emery, B. Rozitis, and M. T. Capria, “Thermophysical modeling of asteroid surfaces,” in *Asteroids IV*, 1–21 (2015).
- [66] M. Delbo, S. Lorigi, A. Matter, A. Cellino, and J. Berthier, “First VLTI-MIDI Direct Determinations of Asteroid Sizes,” *The Astrophysical Journal* **694**, 1228–1236 (2009).
- [67] A. Matter, M. Delbo, B. Carry, and S. Lorigi, “Evidence of a metal-rich surface for the Asteroid (16) Psyche from interferometric observations in the thermal infrared,” *Icarus* **226**, 419–427 (2013).
- [68] A. Matter, M. Delbo, S. Lorigi, N. Crouzet, and P. Tanga, “Determination of physical properties of the Asteroid (41) Daphne from interferometric observations in the thermal infrared,” *Icarus* **215**, 47–56 (2011).
- [69] B. Carry, A. Matter, P. Scheirich, P. Pravec, L. Molnar, S. Mottola, A. Carbognani, E. Jehin, A. Marciniak, R. P. Binzel, F. E. DeMeo, M. Birlan, M. Delbo, E. Barbotin, R. Behrend, M. Bonnardeau, F. Colas, P. Farissier, M. Fauvaud, S. Fauvaud, C. Gillier, M. Gillon, S. Hellmich, R. Hirsch, A. Leroy, J. Manfroid, J. Montier, E. Morelle, F. Richard, K. Sobkowiak, J. Strajnic, and F. Vachier, “The small binary asteroid (939) Isberga,” *Icarus* **248**, 516–525 (2015).
- [70] S. J. Ostro, J.-L. Margot, L. A. M. Benner, J. D. Giorgini, D. J. Scheeres, E. G. Fahnestock, S. B. Broschart, J. Bellerose, M. C. Nolan, C. Magri, P. Pravec, P. Scheirich, R. Rose, R. F. Jurgens, E. M. De Jong, and S. Suzuki, “Radar Imaging of Binary Near-Earth Asteroid (66391) 1999 KW₄,” *Science* **314**, 1276–1280 (2006).
- [71] F. Marchis, P. Descamps, D. Hestroffer, and J. Berthier, “Discovery of the triple asteroidal system 87 Sylvia,” *Nature* **436**, 822–824 (2005).
- [72] F. Marchis, D. Hestroffer, P. Descamps, J. Berthier, C. Laver, and I. de Pater, “Mass and density of Asteroid 121 Hermione from an analysis of its companion orbit,” *Icarus* **178**, 450–464 (2005).
- [73] F. Marchis, M. Kaasalainen, E. F. Y. Hom, J. Berthier, J. Enriquez, D. Hestroffer, D. Le Mignant, and I. de Pater, “Shape, size and multiplicity of main-belt asteroids. I. Keck Adaptive Optics survey,” *Icarus* **185**, 39–63 (2006).
- [74] F. Marchis, D. Hestroffer, P. Descamps, J. Berthier, A. H. Bouchez, R. D. Campbell, J. C. Y. Chin, M. A. van Dam, S. K. Hartman, E. M. Johansson, R. E. Lafon, D. Le Mignant, I. de Pater, P. J. Stomski, D. M. Summers, F. Vachier, P. L. Wizinovich, and M. H. Wong, “A low density of 0.8gcm⁻³ for the Trojan binary asteroid 617Patroclus,” *Nature* **439**, 565–567 (2006).
- [75] P. Descamps, F. Marchis, T. Michalowski, F. Vachier, F. Colas, J. Berthier, M. Assafin, P. B. Dunckel, M. Polińska, W. Pych, D. Hestroffer, K. P. M. Miller, R. Vieira-Martins, M. Birlan, J. P. Teng-Chuen-Yu, A. Peyrot, B. Payet, J. Dorseuil, Y. Léonie, and T. Dijoux, “Figure of the double Asteroid 90 Antiope from adaptive optics and lightcurve observations,” *Icarus* **187**, 482–499 (2007).

- [76] P. Descamps, F. Marchis, T. Michalowski, F. Colas, J. Berthier, F. Vachier, J. P. Teng-Chuen-Yu, A. Peyrot, B. Payet, J. Dorseuil, Y. Léonie, T. Dijoux, H. Berrouachdi, C. Chion Hock, and F. Benard, “Nature of the small main belt Asteroid 3169 Ostro,” *Icarus* **189**, 362–369 (2007).
- [77] P. Descamps, F. Marchis, J. Pollock, J. Berthier, F. Vachier, M. Birlan, M. Kaasalainen, A. W. Harris, M. H. Wong, W. J. Romanishin, E. M. Cooper, K. A. Kettner, P. Wiggins, A. Kryszczyńska, M. Polińska, J. F. Coliac, A. Devyatkin, I. Verestchagina, and D. Gorshanov, “New determination of the size and bulk density of the binary Asteroid 22 Kalliope from observations of mutual eclipses,” *Icarus* **196**, 578–600 (2008).
- [78] P. Scheirich and P. Pravec, “Modeling of lightcurves of binary asteroids,” *Icarus* **200**, 531–547 (2009).
- [79] J. Durech, B. Carry, M. Delbo, M. Kaasalainen, and M. Viikinkoski, “Asteroid Models from Multiple Data Sources,” in *Asteroids IV*, University of Arizona Press, Tucson, AZ (2015).
- [80] M. Wittkowski, Y. Balega, T. Beckert, W. J. Duschl, K.-H. Hofmann, and G. Weigelt, “Diffraction-limited 76mas speckle masking observations of the core of NGC 1068 with the SAO 6m telescope,” *A&A* **329**, L45–L48 (1998).
- [81] G. Weigelt, M. Wittkowski, Y. Y. Balega, T. Beckert, W. J. Duschl, K.-H. Hofmann, A. B. Men’shchikov, and D. Schertl, “Diffraction-limited bispectrum speckle interferometry of the nuclear region of the Seyfert galaxy NGC 1068 in the H and K’ bands,” *A&A* **425**, 77–87 (2004).
- [82] M. Wittkowski, P. Kervella, R. Arsenault, F. Paresce, T. Beckert, and G. Weigelt, “VLTI/VINCI observations of the nucleus of NGC 1068 using the adaptive optics system MACAO,” *A&A* **418**, L39–L42 (2004).
- [83] W. Jaffe, K. Meisenheimer, H. J. A. Röttgering, C. Leinert, A. Richichi, O. Chesneau, D. Fraix-Burnet, A. Glazenberg-Kluttig, G.-L. Granato, U. Graser, B. Heijligers, R. Köhler, F. Malbet, G. K. Miley, F. Paresce, J.-W. Pel, G. Perrin, F. Przygodda, M. Schoeller, H. Sol, L. B. F. M. Waters, G. Weigelt, J. Woillez, and P. T. de Zeeuw, “The central dusty torus in the active nucleus of NGC 1068,” *Nature* **429**, 47–49 (2004).
- [84] N. López-Gonzaga, W. Jaffe, L. Burtscher, K. R. W. Tristram, and K. Meisenheimer, “Revealing the large nuclear dust structures in NGC 1068 with MIDI/VLTI,” *A&A* **565**, A71 (2014).
- [85] K. R. W. Tristram, K. Meisenheimer, W. Jaffe, M. Schartmann, H.-W. Rix, C. Leinert, S. Morel, M. Wittkowski, H. Röttgering, G. Perrin, B. Lopez, D. Raban, W. D. Cotton, U. Graser, F. Paresce, and T. Henning, “Resolving the complex structure of the dust torus in the active nucleus of the Circinus galaxy,” *A&A* **474**, 837–850 (2007).
- [86] K. R. W. Tristram, L. Burtscher, W. Jaffe, K. Meisenheimer, S. F. Hönl, M. Kishimoto, M. Schartmann, and G. Weigelt, “The dusty torus in the Circinus galaxy: a dense disk and the torus funnel,” *A&A* **563**, A82 (2014).
- [87] K. Meisenheimer, K. R. W. Tristram, W. Jaffe, F. Israel, N. Neumayer, D. Raban, H. Röttgering, W. D. Cotton, U. Graser, T. Henning, C. Leinert, B. Lopez, G. Perrin, and A. Prieto, “Resolving the innermost parsec of Centaurus A at mid-infrared wavelengths,” *A&A* **471**, 453–465 (2007).
- [88] L. Burtscher, K. Meisenheimer, W. Jaffe, K. R. W. Tristram, and H. J. A. Röttgering, “Resolving the Nucleus of Centaurus A at Mid-Infrared Wavelengths,” *Publ. of the Astron. Soc. of Australia* **27**, 490–495 (2010).
- [89] G. Weigelt, K.-H. Hofmann, M. Kishimoto, S. Hönl, D. Schertl, A. Marconi, F. Millour, R. Petrov, D. Fraix-Burnet, F. Malbet, K. Tristram, and M. Vannier, “VLTI/AMBER observations of the Seyfert nucleus of NGC 3783,” *A&A* **541**, L9 (2012).
- [90] L. Burtscher, K. Meisenheimer, K. R. W. Tristram, W. Jaffe, S. F. Hönl, R. I. Davies, M. Kishimoto, J.-U. Pott, H. Röttgering, M. Schartmann, G. Weigelt, and S. Wolf, “A diversity of dusty AGN tori. Data release for the VLTI/MIDI AGN Large Program and first results for 23 galaxies,” *A&A* **558**, A149 (2013).
- [91] R. G. Petrov, F. Millour, S. Lagarde, M. Vannier, S. Rakshit, A. Marconi, and G. weigelt, “VLTI/AMBER differential interferometry of the broad-line region of the quasar 3C273,” in *Optical and Infrared Interferometry III, Proc. SPIE* **8445**, 84450W (2012).
- [92] J. H. Krolik and M. C. Begelman, “Molecular tori in Seyfert galaxies - Feeding the monster and hiding it,” *ApJ* **329**, 702–711 (1988).
- [93] M. Nenkova, Ž. Ivezić, and M. Elitzur, “Dust Emission from Active Galactic Nuclei,” *ApJ* **570**, L9–L12 (2002).

- [94] M. Schartmann, K. Meisenheimer, M. Camenzind, S. Wolf, and T. Henning, “Towards a physical model of dust tori in Active Galactic Nuclei. Radiative transfer calculations for a hydrostatic torus model,” *A&A* **437**, 861–881 (2005).
- [95] S. F. Hönig, T. Beckert, K. Ohnaka, and G. Weigelt, “Radiative transfer modeling of three-dimensional clumpy AGN tori and its application to NGC 1068,” *A&A* **452**, 459–471 (2006).
- [96] M. Schartmann, K. Meisenheimer, M. Camenzind, S. Wolf, K. R. W. Tristram, and T. Henning, “Three-dimensional radiative transfer models of clumpy tori in Seyfert galaxies,” *A&A* **482**, 67–80 (2008).